A TECHNIQUE FOR MEASURING THE DISPLACEMENT VECTOR THROUGHOUT THE BODY OF A PAVEMENT STRUCTURE SUBJECTED TO CYCLIC LOADING

William M. Moore and Gilbert Swift, Texas Transportation Institute,
Texas A&M University

•THIS is a progress report on phase 2 of a research study entitled Design and Evaluation of Flexible Pavements, which is being conducted by the Texas Transportation Institute and sponsored by the Texas Highway Department and the Federal Highway Administration. The objective of this phase of the research, as quoted from the study proposal, is "to develop from full-scale testing, a mathematical model estimating the displacement vector at any given point within a pavement structure subjected to Dynaflect loading, given this vector at the surface, the thickness of each layer and a stiffness parameter for each material." Two different models for estimating the vertical component of the displacement vector on a pavement's surface were developed in previous publications (1, 2). The second and more accurate model was used in the development of the flexible pavement design system (3), which is being expanded and implemented in study 123 (4). Use of this model has pointed out several weak points and a pressing need for a still more accurate one.

An accurate model for predicting the displacement vector within any given pavement structure will provide design engineers with a means of calculating strains within the structure and will be an important step in the development of a more realistic approach to pavement design. Thus, it is expected that this study will represent a significant step toward obtaining a more rational pavement design theory.

Several researchers have reported measurements of stresses and strains in situ (5, 6, 7, 8). However, placing stress or strain sensors within a pavement structure tends to destroy the continuity of the material and therefore alters the distribution of the quantities being measured. In contrast, displacement measurements should be substantially unaffected by small perturbations of the system.

Any displacement measurement requires a reference point. As pointed out elsewhere (9), the Dynaflect technique of applying a cyclic force makes it possible to employ an inertial reference point that is not susceptible to measurement errors caused by reference point motion. Other methods of measuring displacement require a physical, tangible reference point that must be sufficiently remote to remain undisturbed during the measurement, at least to the extent set by the desired accuracy of the measurement. Such a point would be quite deep or quite far away if on the surface. Thus, the measurement would require the determination of an extremely small change in a relatively large distance, a requirement that is believed to lead to unacceptably large errors. Accordingly an extention of the Dynaflect measuring technique, employing geophones as displacement sensors, was adopted for this study.

Surface deflections of a pavement structure, as normally measured with the Dynaflect, provide insufficient data to define the response of the entire structure to the loading on its surface. Thus, measurement of the displacement vector field throughout the pavement structure was undertaken in this study to provide data for developing the model required in the study's objective or for verifying existing models such as linear elasticity, linear viscoelasticity, and so forth.

Sponsored by Committee on Pavement Condition Evaluation.

The purpose of this report is to describe the apparatus and technique developed to measure both horizontal and vertical components of the displacement vector. It includes typical measurements obtained as well as the replication errors encountered.

SCOPE OF MEASUREMENTS PROGRAM

The Texas A&M pavement test facility is being used to obtain data for analysis. This facility, located at the University's Research Annex, was constructed for the purpose of providing a means for evaluating nondestructive testing techniques and especially for evaluating testing equipment purporting to furnish information concerning the in situ characteristics of the individual layers in a flexible pavement. It consists of 32, 12- by 40-ft test sections that have different structural characteristics in accordance with the principles of statistical experiment design. The design of the facility is described in detail elsewhere (1). Plan and cross-sectional views of the test facility are shown in Figure 1.

The displacement vector field of a test section is induced by loading the section with a Dynaflect. This instrument, shown in Figure 2, produces a vertical dynamic load of 1,000 lb, oscillating sinusoidally with time at 8 Hz, which is applied to the surface through two steel wheels spaced 20 in. apart. A complete description is given elsewhere (9, 10). Vertical displacement measurements are made on the surface of the pavement by using low-frequency geophones whose output voltage is directly proportional to the amplitude of the sinusoidal motion.

The displacement vector field was determined on a test section by measuring separately the horizontal and vertical components of motion at selected depths and horizontal distances from the points of application of the surface loads. Individual component measurements were made by using a miniature geophone—either one designed for horizontal motion or one designed for vertical motion. The geophone was clamped in place in a small-diameter hole drilled vertically in the pavement section. The measurement depth was altered by clamping the geophone at various depths, while the horizontal distance from the points of application of the surface load was altered by moving the Dynaflect forward on the surface various distances. By utilizing this concept (Fig. 3), we made sufficient measurements to define both the vertical and horizontal component fields in the region from 0 to about 5 ft in depth and from approximately 1 to 18 ft in horizontal distance. Because of the 20-in. spacing of the Dynaflect load wheels, it was not practical to make measurements at horizontal distances less than 10 in.

To date, displacement vector fields have been measured at two locations on each of three test sections. The planned program includes replicate measurements on all 32 of the test sections. Replicate measurements, made on opposite ends of each test section, will permit analysis of overall precision. Replication errors observed on a test section not only reflect the variability of the measuring process but also include the effects of variations in the structural properties of the section. The combined variability will define the limiting prediction accuracy for the displacement model being sought.

MEASURING TECHNIQUE

Basic Technique

Extension of the Dynaflect technique to the measurements of the displacement vector throughout the pavement structure was accomplished by using a pair of suitable geophones—one responsive only to the vertical component of motion, the other responsive only to the horizontal component—and clamping them one at a time at selected depths in a single hole in the structure. With either geophone placed at a given depth, the Dynaflect was positioned at a succession of locations on the surface ranging from directly above the hole up to 18 ft away.

Geophone Emplacement

In order to minimize disturbance to the pavement sections, we obtained miniature geophones, and an assembly that could be emplaced was designed. The assembly was

Figure 1. Pavement test facility.

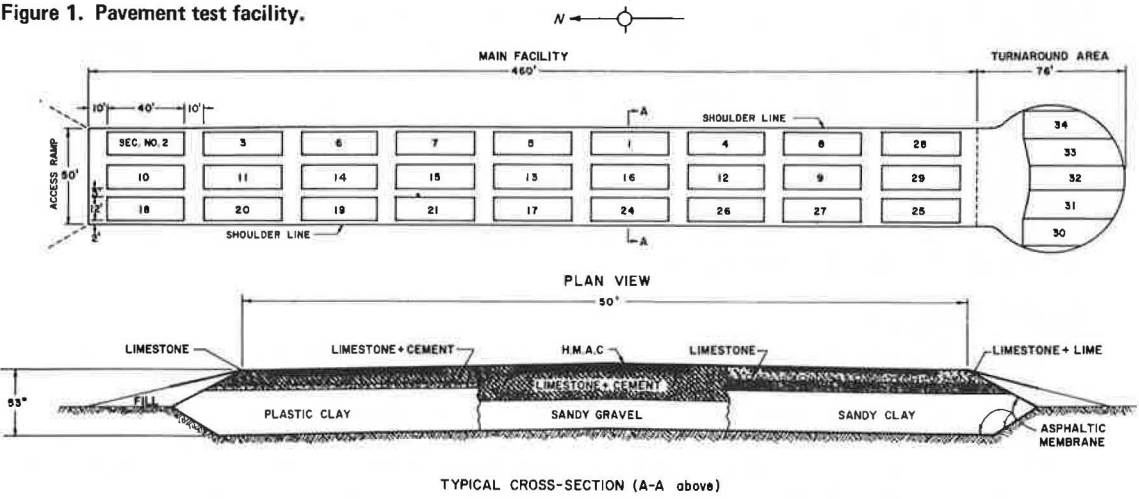

TYPICAL CROSS-SECTION (A-A above)

Figure 2. Dynaflect trailer in normal use with five-geophone array on pavement surface.

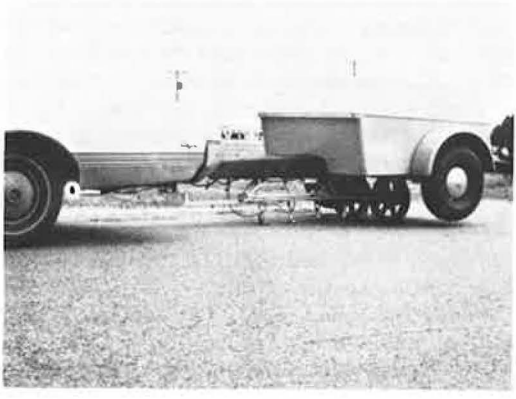

Figure 3. Representation of the technique used to measure vector displacements within a pavement section.

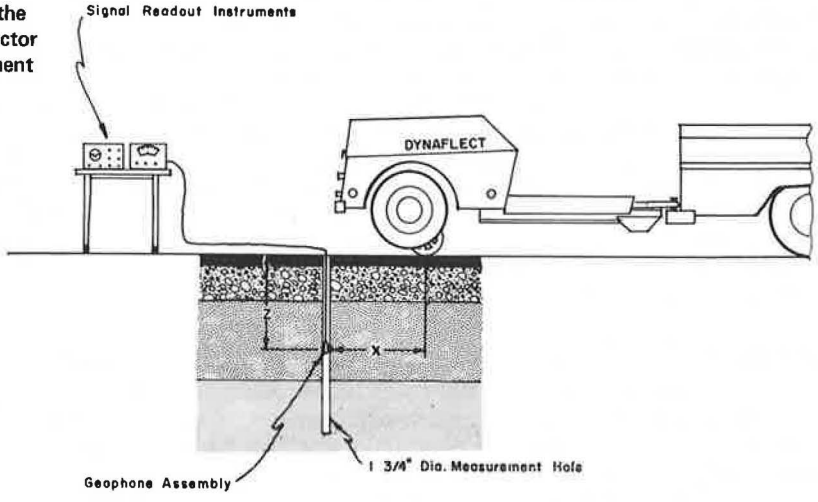

sufficiently small to fit within a $1\frac{3}{4}$-in. diameter hole. The down-hole geophone assembly is shown in Figure 4. It contains a waterproof aluminum housing in which one geophone, either horizontal or vertical, is mounted. Two spring-loaded pistons can be released to expand outward and clamp the device in the hole. Flexible steel cables (fishing leader wire) extend above the surface to permit the release and retraction of the pistons. A removable hollow rod, through which the electrical output cable passes, allows the $1\frac{5}{8}$-in. diameter device to be lowered into the hole with the pistons retracted. At the desired depth, the pistons are released. The rod is then disconnected and removed from the hole, leaving the unit in place with slack wires extending to the surface. The unit is retrieved by reversing this procedure.

Drilling Technique

After disappointing results were obtained with several types of drill rigs and drill bits, a satisfactory combination was found. All of the successful holes, usable for geophone emplacement, have been drilled with a Clipper Core Drill Model D-30-P using a diamond core barrel, $1\frac{3}{4}$ in. in diameter and 14 in. long. This drill is used with a continuous flow of compressed air while penetrating the hot-mix asphaltic concrete surface layer and the limestone base or subbase layers. The same core barrel is employed, without airflow, to penetrate the softer embankment and subgrade materials. Where the material is soft clay, the drill is used without rotation.

It was decided before undertaking this work that air must be employed during drilling because water would alter or damage the pavement sections. In spite of this precaution, water trapped in the embankment material invaded several of the holes during the measurement period within 1 or 2 hours after hole completion. No adverse effects were attributable to this water in those sections in which it was possible to complete the measurement sequence. In one group of sections, however, the hole walls collapsed and prevented emplacement of the geophone. It is planned to drain the excess water from the saturated zones prior to making more measurements on these sections.

Measuring Procedure

The measuring procedure developed for this investigation began with emplacement of the vertical geophone at the greatest chosen depth. The Dynaflect was then positioned on the surface directly over the hole. After it read and recorded the geophone output voltage, the Dynaflect was moved away from the hole to each of a series of preselected distances. The geophone signal was read and recorded at each location. At the end of each such series of measurements, the geophone was retrieved and repositioned at a shallower depth in the hole. On completion of the entire grid of measurements, the preceding procedure was repeated using the horizontal geophone. When using the latter, in addition to recording the magnitude of its output signal, the phase angle was observed to determine whether the horizontal displacement was toward or away from the load.

Ordinarily, one hole and one entire set of vertical and horizontal displacement measurements can be completed within a day. At the end of each set of horizontal or vertical measurements, the geophone used for that set was calibrated by observing its response to a 0.005-in. oscillatory motion provided by the Dynaflect calibrator unit. The calibration factor thus established was utilized to convert the recorded voltage readings to displacements in millionths of an inch. By using a Hewlett Packard Model 502A Wave Analyzer to read the voltages, we measured displacements as small as a millionth of an inch. Thus far, the observed movements have ranged from less than 1 millionth to 2 thousandths of an inch.

Transformation of Measurements to a Single Load Vector Field

As previously mentioned, the Dynaflect applies a 1,000-lb load to the surface through two wheels that are spaced 20 in. apart. Hence, when the Dynaflect is centered over a hole, its two load application points are equidistant at a 10-in. radial (horizontal) distance from the hole. Moving the Dynaflect forward a distance, x, along a straight line increases both of these radial distances while maintaining their equality. The radial distance, r, from the hole to either of the load application points is given by

$$r = \sqrt{x^2 + 10^2}$$

In order to simplify the presentation of the data, we converted the observed measurements to the case of a single 1,000-lb axially symmetrical load acting at a distance, r, from the hole by assuming that the displacement vectors at any depth, z, produced by the two 500-lb loads were of equal magnitude and were vectorially additive.

The vertical displacement components produced by each of the two loads are alike in both magnitude and direction; therefore, the vertical component for a single 500-lb load would be half the measured value, and for a single 1,000-lb load it would be equal to the measured value. This measured value is represented by the symbol w.

The horizontal components of motion produced by each load wheel are alike in magnitude but, unlike the vertical components, are directed along lines parallel to the radial (horizontal) lines on the surface joining the hole with the individual load application points. Hence, when the Dynaflect is centered over the hole, the horizontal components due to each load wheel are in opposite directions. Because this represents a null of horizontal motion, the horizontal measurement is omitted at this position. The horizontal measurement closest to the loads is made with the Dynaflect axle 6 in. away from the hole, and the most remote measurement is made when it is 18 ft (or 216 in.) away. At any given forward distance x (Fig. 5), the horizontal displacement components produced by each load wheel are equal in magnitude but are separated by an angle 2α, where $\alpha = \arctan(10/x)$. Thus the measured horizontal displacement, M_h, is related to the horizontal displacement, u, resulting from a single 1,000-lb load, by

$$u = M_h \sec \alpha$$

as is verified by Figure 5.

Sec α can be regarded as a correction factor that is applied to the measured values of horizontal displacement to transform them to values that would have been obtained in the assumed axially symmetrical case. Figure 6 shows sec α versus x. From this plot, it can be seen that the correction factor approaches unity very quickly as the Dynaflect is moved forward to increase the horizontal distance x. Thus, the principle of Saint-Venant is illustrated in that the correction factor becomes insignificant at values of x exceeding two or three times the 20-in. distance between the load wheels (11).

GEOMETRIC LIMITS OF VECTOR FIELD

Because the existing dimensions of the Dynaflect make it inconvenient to measure vertical displacements at locations closer than x = 0 (or r = 10 in.) from the load application points or horizontal displacements at locations closer than x = 6 in. (or r = 11.7 in.), these dimensions form the close-in limits of the measured displacement fields. The far-out limit of x = 216 in. (or r = 216.2 in.) was selected on consideration of the finite (40 ft) length of the sections and the observed diminution of the displacements with distance and with depth. The depth limit, at $z \approx 65$ in. below the surface, was selected on the basis that the test facility comprises 53 in. of selected materials situated on a reasonably uniform clay foundation that is regarded as extending infinitely downward. In view of the observed displacement behavior, it is believed that the outer limits of the measured fields have been placed amply far to encompass the region of major interest and to permit reasonable extrapolation beyond this region.

Thus, the geometrical limits of the transformed vector fields determined from the measurements are as follows:

1. Field of the component u—11.7 in. $\leq r \leq$ 216.2 in., $0 \leq z \leq 65$ in. (approximately), and
2. Field of the component w—10 in. $\leq r \leq$ 216.2 in., $0 \leq z \leq 65$ in. (approximately).

MEASURED DISPLACEMENTS

Replicate measurements of displacements have been made on three pavement sections and are shown for one section in Figures 7 and 8. Single sets of measurements for the

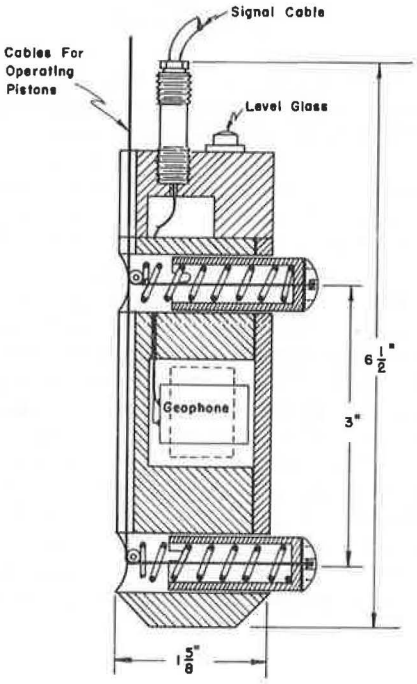

Figure 4. Cross-sectional view of subsurface geophone assembly.

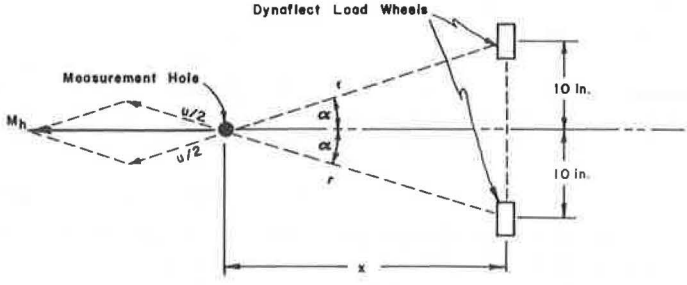

Figure 5. Relation of the horizontal displacement vectors produced by each load wheel and the measured horizontal displacement.

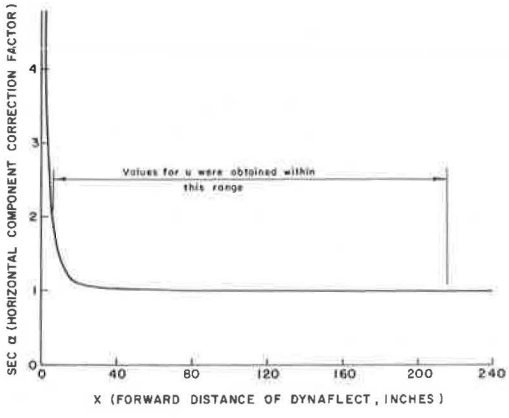

Figure 6. Relation of forward distance of Dynaflect and correction factor applied to the measured horizontal displacement in the transformation to a single load point.

Figure 7. Displacement fields measured in section 25—numerical values on contours denote displacements in microinches.

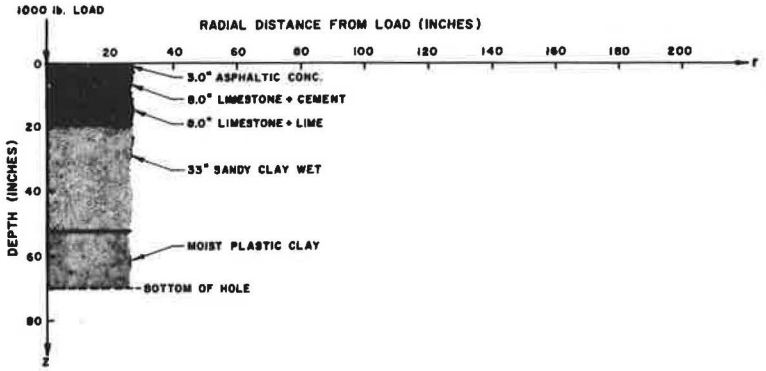

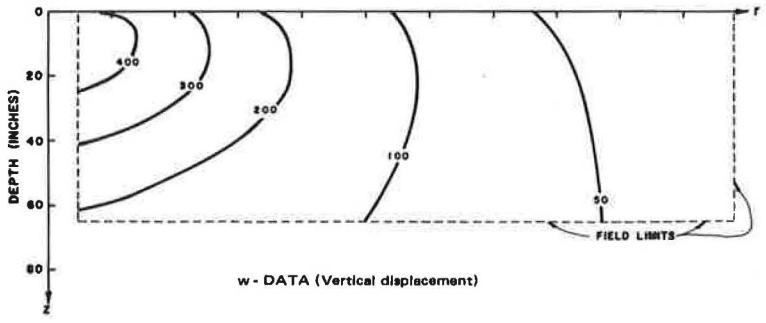

w - DATA (Vertical displacement)

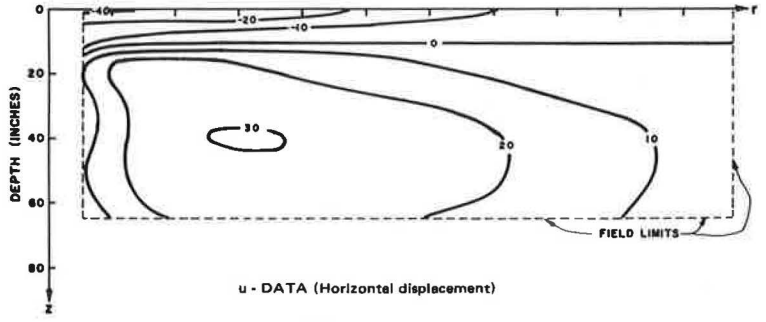

u - DATA (Horizontal displacement)

REPLICATION 1

Figure 8. Replicate measurements of section 25 at a location 40 feet away from the location used for Figure 7.

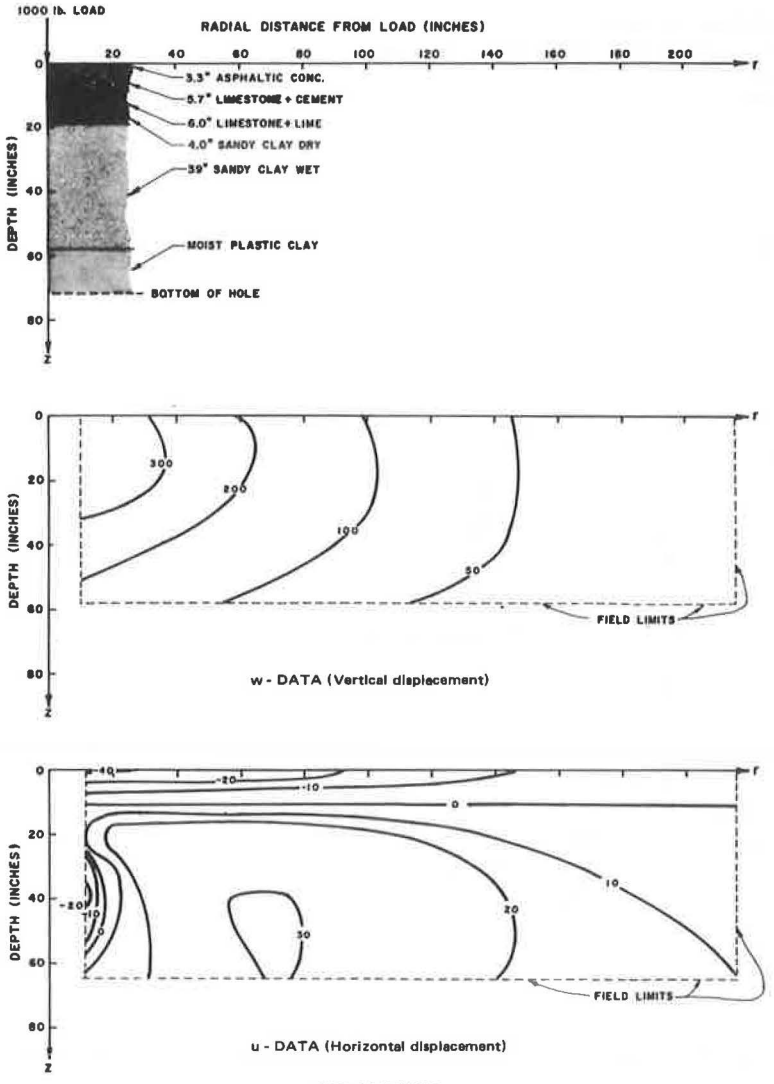

REPLICATION 2

Figure 9. Displacement fields measured in section 31—numerical values on contours denote displacements in microinches.

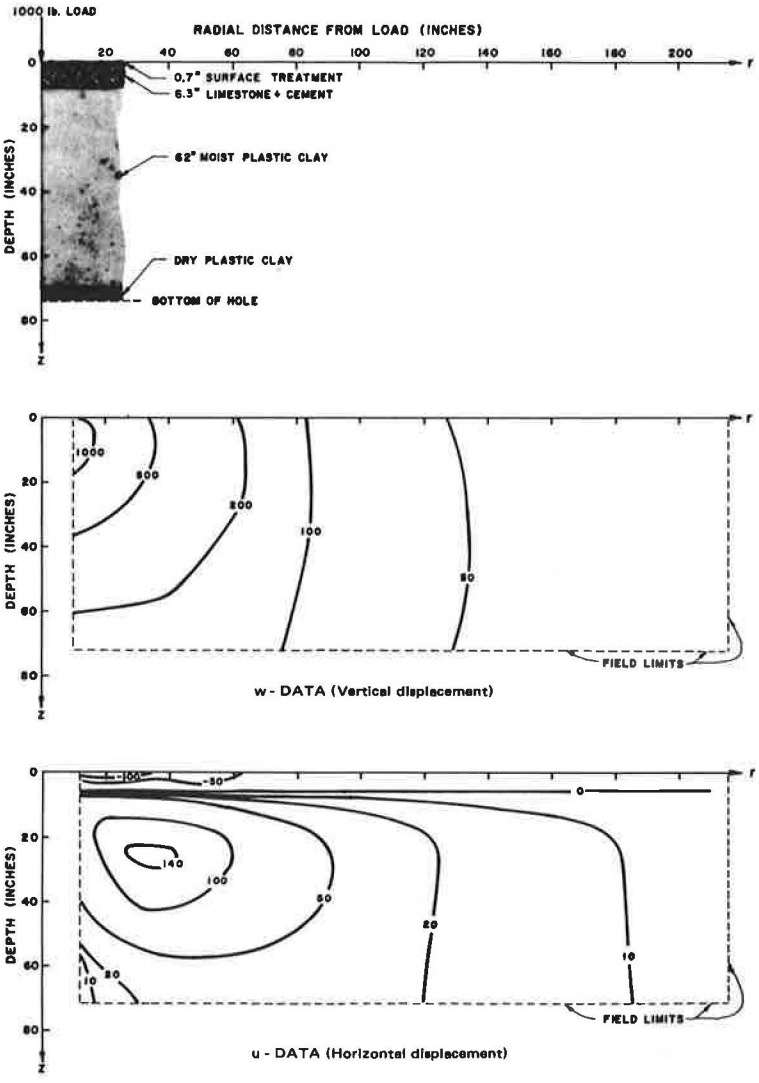

REPLICATION 1

Figure 10. Displacement fields measured in section 32—numerical values on contours denote displacements in microinches.

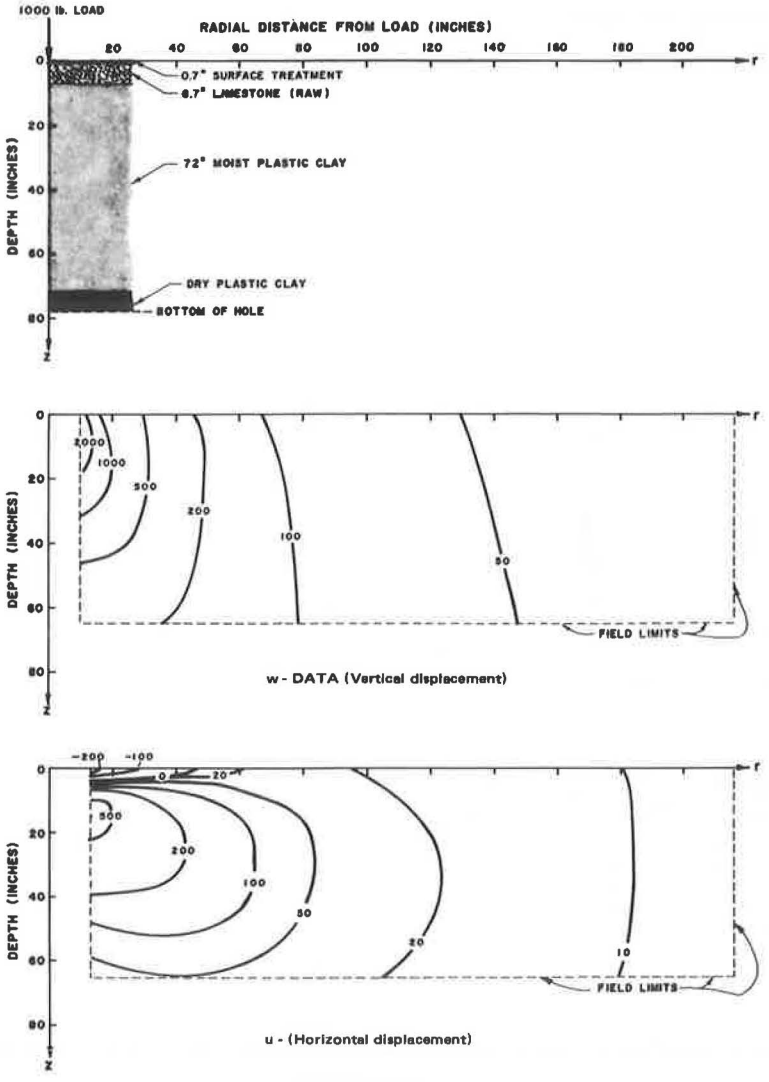

REPLICATION 1

other two sections are shown in Figures 9 and 10. In each of these figures, the layer thicknesses determined in the measurement holes are shown at the top, contours of equal vertical displacement, w, are shown in the center, and contours of equal horizontal displacement, u, are shown at the bottom. Typical data used to prepare these figures are given in the Appendix.

Observed w values are positive everywhere in all plots; thus all points had a component of motion downward. Both positive and negative values were found for u. Positive values indicate a component of motion directed outward from the load axis; negative values indicate motion toward it.

For all three sections, the fields obtained for replication 1 are very similar to those for replication 2. The differences between the replications are quite small in comparison to the differences between sections. The main difference between sections that can be seen in the w fields is in the magnitude near the load. More striking differences between sections appear in the u fields. The general magnitude of the displacements in the three sections shown is clearly related to the designs; that is, the magnitudes are in inverse order of pavement strength.

Figure 11 shows w and u fields for a two-layer elastic system that is composed of a 19-in. thick top layer having an elastic modulus of 600,000 psi above an infinitely thick layer having an elastic modulus of 20,000 psi with Poisson's ratio equal to 0.5 in both layers. The dimension of 19 in. was chosen to match the total design pavement thickness (depth to top of embankment) of section 25. The displacements shown were calculated by using a computer program developed by the Chevron Oil Company (12, 13) using a 1,000-lb load on a circular area having a radius of 1.41 in. This radius approximates that of the contact area of a Dynaflect load wheel (14).

The measurements made on section 25 (Figs. 7 and 8) are somewhat similar to the fields computed for the two-layer elastic system shown in Figure 11. The general shapes of both the u and the w fields are alike, and the position of the zero contour for u in both cases is approximately horizontal and about 10 in. from the pavement surface. Work toward developing elastic-layered system fields to match the observed fields is continuing.

REPLICATION ERRORS

As previously mentioned, replicate measurements were made on opposite ends of a test section, and their differences generally were found to be quite small when compared with differences among sections, as evidenced by Figures 8, 9, and 10. The differences among the measurements made on the same section are due to both the variability of the measuring process and the variability in the structural characteristics of the section at its two ends. In the measurement procedure used, all points were not replicated. Thus, in the determination of the replication errors, only the points that were replicated could be compared.

Plots of the replication errors for section 25 (half the difference between the observations) versus the mean observation (half the sum of the observations) are shown in Figure 12. Also shown on these plots are the percentage-of-error lines that include three-fourths of the replication errors. As can be seen in these figures, the data are somewhat biased as indicated by the sloping trend of the w points. This indicates a consistent difference between the two ends of the section. Nevertheless, when disregarding the reasons for the errors, the errors found in w are very small when compared to the range of the measured values, and the errors found in u are thought to be acceptable. The larger percentage of errors found in u are chiefly due to the fact that the relative magnitude of u changes much more rapidly within the measured field than does the relative magnitude of w. This is evidenced by the crowding of the contour lines in the plots of the u fields (Figs. 7, 8, 9, and 10).

Table 1 gives a summary of the replication measurements. It shows the average, the average absolute, and the range of the mean observations. From these values, one can note that the sections measured were very different. The table also contains the maximum absolute and the root mean square of the replication errors as well as the percentage-of-error values that include half and three-fourths of the errors. Values from the last column for section 25 are shown in Figure 12.

Figure 11. Computed displacement fields for two-layered elastic system—numerical values on contours denote displacements in microinches.

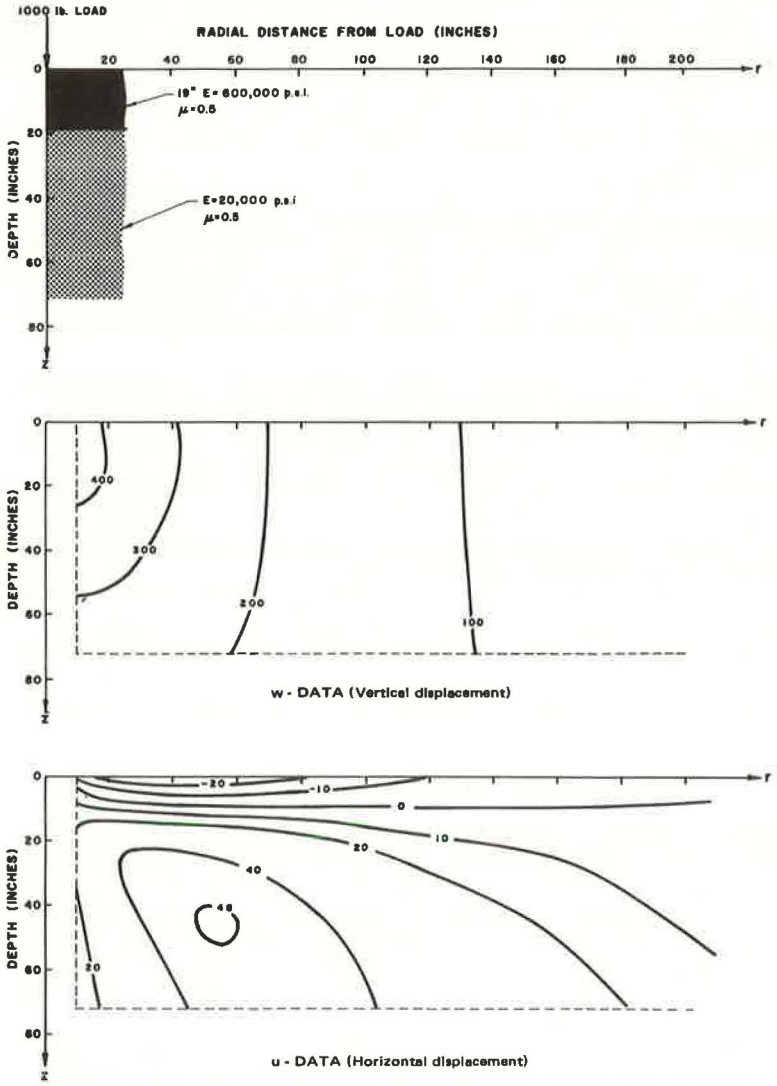

Figure 12. Replication errors for section 25 (half the difference between observations) versus mean observations—scales are in microinches and multiple occurrences of points are indicated by number.

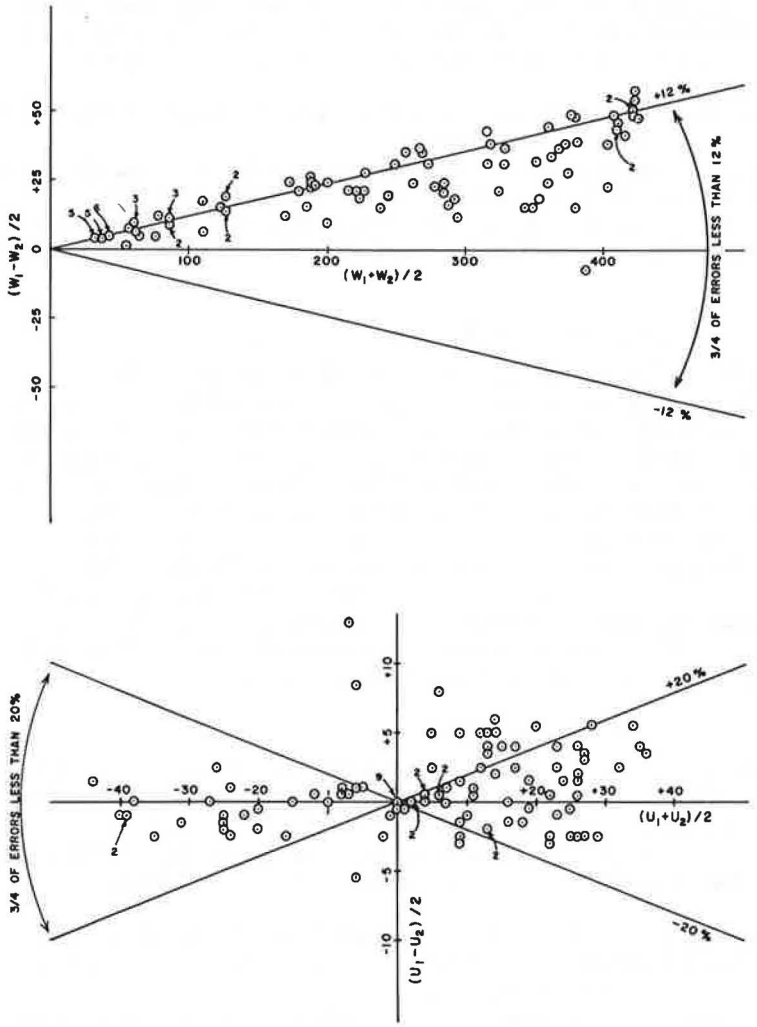

Table 1. Summary of replication measurements.

Section	Variable Measured	Number of Comparisons	Mean Observation[a]			Replication Error[b]		Percentage of Error[c]	
			Average	Average Absolute	Range	Maximum Absolute	Root Mean Square	½ of Errors	¾ of Errors
25	w	98	223.6	223.6	31 to 424	57	26.4	10	12
25	u	104	4.1	15.6	-44 to 36	13	2.9	10	20
31	w	196	301.4	301.4	30 to 1,545	303	52.8	5	8
31	u	182	33.4	51.3	-210 to 166	97	13.6	10	19
32	w	112	433.9	433.9	30 to 2,912	307	60.9	3	6
32	u	89	94.6	123.4	-686 to 556	126	34.0	13	20

[a]Mean of two replicated observations, $(w_1 + w_2)/2$ or $(u_1 + u_2)/2$.
[b]One-half of the difference between two replicated observations, $(w_1 - w_2)/2$ or $(u_1 - u_2)/2$.
[c]Replication error divided by mean observation and expressed as a percentage.

CONCLUSIONS

The results of this study support the following conclusions:

1. A practical fieldworthy measuring technique has been developed for use with the Dynaflect to observe the displacement vector throughout the body of a pavement section;
2. Replication errors observed on a test section are reasonably small compared to variations between sections;
3. The observed vector displacement fields resemble fields computed for a layered elastic system to which an equal static load is applied;
4. It appears feasible to determine for each section a set of elastic layers for which the computed displacement fields will substantially match the observations; and
5. Examination of the data indicates that it should be possible to formulate a useful and practical mathematical model representing the displacement response of the several pavement sections.

ACKNOWLEDGMENTS

The research was done by the Texas Transportation Institute, Texas A&M University, in cooperation with the Texas Highway Department and was sponsored jointly by the Texas Highway Department and the Federal Highway Administration. The authors wish to thank all members of the Institute who assisted in this research. They would like to express special appreciation to Frank H. Scrivner and Lionel J. Milberger. Their help throughout the study has been particularly valuable. Thanks are also due C. H. Michalak for his assistance in the data reduction phase and John Salyer for his assistance during the fabrication and testing phases. The authors are grateful to the Texas Highway Department for its interest and cooperation. They would like to express special gratitude to James L. Brown and Larry J. Buttler of the Highway Design Division for their assistance and support of this research and to the personnel of Districts 8 and 17 for their assistance during the development of the drilling technique.

REFERENCES

1. Scrivner, F. H., and Moore, W. M. Evaluation of the Stiffness of Individual Layers in a Specially Designed Pavement Facility From Surface Deflections. Texas Transportation Institute, Texas A&M Univ., Res. Rept. 32-8, 1966.
2. Scrivner, F. H., and Moore, W. M. An Empirical Equation for Predicting Pavement Deflections. Texas Transportation Institute, Texas A&M Univ., Res. Rept. 32-12, 1968.
3. Scrivner, F. H., Moore, W. M., McFarland, W. F., and Carey, G. R. A Systems Approach to the Flexible Pavement Design Problem. Texas Transportation Institute, Texas A&M Univ., Res. Rept. 32-11, 1968.
4. Hudson, W. R., McCullough B. F., Scrivner, F. H., and Brown, J. L. A Systems Approach Applied to Pavement Design and Research. Texas Transportation Institute, Texas A&M Univ., Res. Rept. 123-1, 1970.
5. Brown, S. F., and Pell, P. S. An Experimental Investigation of the Stresses, Strains, and Deflections in a Layered Pavement Structure Subjected to Dynamic Loads. Proc. 2nd Internat. Conf. on Structural Design of Asphalt Pavements, Univ. of Michigan, Ann Arbor, 1967, pp. 487-504.
6. Busfeldt, K. H., and Dempwolff, K. R. Stress and Strain Measurements in Experimental Road Sections Under Controlled Loading Conditions. Proc. 2nd Internat. Conf. on Structural Design of Asphalt Pavements, Univ. of Michigan, Ann Arbor, 1967, pp. 663-669.
7. Klomp, A. J. G., and Niesman, T. W. Observed and Calculated Strains at Various Depths in Asphalt Pavements. Proc. 2nd Internat. Conf. on Structural Design of Asphalt Pavements, Univ. of Michigan, Ann Arbor, 1967, pp. 671-688.
8. Nijboer, L. W. Testing Flexible Pavements Under Normal Traffic Loadings by Means of Measuring Some Physical Quantities Related to Design Theories. Proc. 2nd Internat. Conf. on Structural Design of Asphalt Pavements, Univ. of Michigan, Ann Arbor, 1967, pp. 689-705.

9. Scrivner, F. H., Swift, G., and Moore, W. M. A New Research Tool for Measuring Pavement Deflection. Highway Research Record 129, 1966, pp. 1-11.
10. Pace, G. M. Evaluation of the Dynaflect for the Non-Destructive Testing of Portland Cement Concrete Pavements. Department of the Army, Ohio Division Laboratories, Corps of Engineers, Cincinnati, Tech. Rept. 4-61, 1967.
11. Timoshenko, S., and Goodier, J. N. Theory of Elasticity. McGraw-Hill Book Co., Inc., 1951, pp. 337-365.
12. Michelow, J. Analysis of Stresses and Displacements in an N-Layered Elastic System Under a Load Uniformly Distributed Over a Circular Area. California Research Corporation, Richmond, Sept. 1963.
13. Warren, H., and Dieckmann, W. L. Numerical Computation of Stresses and Strains in a Multiple-Layered Asphalt Pavement System. California Research Corporation, Richmond, Sept. 1963.
14. Scrivner, F. H., Michalak, C. H., and Moore, W. M. Calculation of the Elastic Moduli of a Two Layer Pavement System From Measured Surface Deflections. Texas Transportation Institute, Texas A&M Univ., Res. Rept. 123-6, 1971.

APPENDIX

TYPICAL REPLICATION DATA

SECTION 25 REPLICATION 1

W - DATA (MICRO-INCHES) FOR SINGLE 1000 LB. LOAD

DEPTH Z (IN.)	**********	RADIAL DISTANCE R (IN.)											**********
	10.0	11.7	15.6	20.6	26.0	37.4	49.0	60.8	72.7	96.5	120.4	144.3	180.3	216.2
0.0	378	424	393	363	357	306	263	209	181	118	81	56	40	33
3.0	469	469	454	424	403	354	303	242	212	145	96	69	48	39
11.0	478	475	454	424	399	345	303	242	212	142	93	66	48	36
15.0	469	469	451	424	403	357	303	248	212	145	96	69	48	39
19.0	451	454	439	409	393	345	303	254	215	142	96	69	48	39
29.0	381	381	369	363	357	309	278	236	199	139	96	66	49	39
41.0	303	299	299	290	284	254	224	196	175	127	90	69	45	36
52.0	230	230	224	218	212	196	178	157	139	109	81	63	45	36
65.0	193	193	187	187	187	175	163	145	133	103	81	63	48	36

U - DATA (MICRO-INCHES) FOR SINGLE 1000 LB. LOAD

DEPTH Z (IN.)	**********	RADIAL DISTANCE R (IN.)											**********
	10.0	11.7	15.6	20.6	26.0	37.4	49.0	60.8	72.7	96.5	120.4	144.3	180.3	216.2
0.0		-42	-38	-40	-39	-39	-37	-32	-26	-20	-14	-10	-7	-5
3.0		-24	-22	-25	-26	-26	-26	-23	-21	-18	-11	-7	-5	-4
11.0		-11	-4	-2	0	0	0	0	0	0	0	0	0	0
15.0		8	13	16	17	19	18	16	14	10	6	4	1	0
19.0		9	18	21	24	26	27	25	22	16	11	7	4	1
29.0		2	10	16	20	27	30	30	29	25	19	15	7	4
41.0		5	13	20	25	33	39	39	39	34	28	20	12	7
52.0		3	10	16	21	28	33	35	35	32	26	21	12	8
65.0		5	6	10	14	18	24	25	26	24	19	15	10	7